Analysis of the circumferential bulging capacity and uniformity under different TEC layout and the roll structure in the ETCR

Zhiqiang Xu (xzq@ysu.edu.cn)
Yanshan University
yang hai
Tingsong Yang
Haonan Zhou
Fengshan Du

Research Article

Keywords: Electronic temperature control roll technology, thermoelectric cooler, TEC layout, roll structure, temperature ratchet

Posted Date: April 13th, 2022

DOI: https://doi.org/10.21203/rs.3.rs-1537486/v1

Abstract

Electronic temperature control roll (ETCR) technology is a new roll profile control technology based on the principle of the semiconductor cooling and heating effect. The thermoelectric cooler (TEC) is the core component for controlling roll profiles in this technology. The TEC layout and the roll structure can affect the bulging ability of the roll, the bulging uniformity and the uniformity of the roll temperature field. To research the influence of the TEC layout and the roll structure on these factors, a circumferential finite element model of ETCR is established by the finite element software MSC.MARC, and is verified on the experimental platform of ETCR. After analysis, it was found that increasing the roll diameter or decreasing the diameter of the roll inner hole can increase the bulging ability of the roll, improve the bulging uniformity and weaken the temperature ratchet. Increasing the temperature of TEC or decreasing the single piece influence angle can increase the bulging ability of the roll and improve the temperature ratchet, while the effect of changing the single piece influence angle on the bulging uniformity is larger than that of the temperature of TEC. In view of the difficulty of circumferential uniform bulging when the single piece influence angle is large, a scheme of adding a metal layer of high thermal conductivity material in the roll inner hole is proposed. The results showed that the copper layer has little influence on the bulging ability of the roll and can reduce the circumferential bulging difference.

1. Introduction

The roll profile is an active factor that changes the load-bearing roll gap shapes in the strip rolling process, which further controls the strip flatness. The roll profile control includes the design of the grinding roll profile and the dynamic control of the roll profile. The design of the grinding roll profile can achieve different control functions by designing a specific roll profile curve. Lu et al [1]. designed a third-order CVC roll profile to reduce the axial force of the working roll. Li et al [2]. proposed a design method of a fourth-order CVC roll profile to improve the ability of the mill to control the strip flatness. Cao et al [3]. proposed a varying contact-length backup roll (VCR) to extend the crown control domain of the roll gap shape and improve the lateral stiffness of the mill. Wang et al [4]. proposed an edge variable crown (EVC) roll to control the edge drop in the rolling process. However, the grinding roll profile curve has difficulty changing the roll profile without reprocessing. Furthermore, the design of the grinding roll profile is also a difficult point in the development of new curves. To solve these problems, dynamic control of the roll profile is proposed based on a force or heat source. Masui et al [5]. proposed a variable crown (VC) roll, which can improve the roll profile by adjusting the oil pressure in the hydraulic chamber of the roll. Zhang et al [6]. studied the shape control capability of a dynamic shape roll (DSR) based on hydraulic cylinder control. The results showed that the shape control range of DSR rolling mills was significantly improved compared with that of ordinary rolling mills. However, the hydraulic pressure bulging ability can be affected by the sealing performance of the hydraulic device, and it is difficult to apply it to heavy-duty conditions for a long time. Sumitomo Metal Industries proposed a thermally bulging roll based on electric-heating rods, which can control the roll profile by heating the roll inner wall [7]. It is still in the patent stage. Liu et al. proposed an electromagnetic control roll based on the principle of roll profile

electromagnetic control technology [8]. The results showed that the bulging amount of the roll is approximately dozens of microns. However, the rolls lack the necessary cooling devices in the Sumitomo Metal Industries' and Liu's technologies. The axial temperature of the roll and the stability of the roll profile are not easy to control. Therefore, this paper proposes an electronic temperature control roll (ETCR) based on the principle of the semiconductor cooling and heating effect. A thermoelectric cooler (TEC) can achieve cooling at one end and heating at the other end after the TEC is powered on. Multigroup TEC forms are used on the roll inner wall to produce a multistage controllable electronic temperature control roll profile. Considering the time-domain characteristics of regulation, ETCR can be used to preset the roll profile and dynamically compensate for the worn roll profile.

The roll profile calculation of ETCR involves the calculation of the temperature field. Arif et al. analysed the influence law of an external input thermomechanical load on the loaded thermal roll profile for this kind of problem [9]. According to the external input heat during hot rolling, Zhang et al. proposed a two-dimensional axisymmetric difference model to analyse the transient temperature field of the working roll and solve the corresponding hot roll profile [10]. The model has been compared with the production line and has a good degree of agreement. Park et al. suggested that the factors of increasing the roll crown are heat flux, roll width, and rolling speed in the twin casting rolling process [11]. Benasciutti et al. proposed that periodic heat sources can cause rolls to produce uneven surface thermal distributions and further induce uneven thermal stresses [12]. Jiang et al. proposed a precision online model of a thermal crown, which can consider the influence of external periodic cooling and rolling heat input [13]. Chen et al. established a finite difference model that can be used to calculate the temperature field of rolls online and pointed out that the adjustment range of the thermal crown as a function of the working roll shifting is approximately ± 30 μm [14]. The above studies have carried out detailed studies on the influence of the temperature field on the hot roll profile, but the circumferential boundaries are simplified to axisymmetric conditions to facilitate the solution. Therefore, the studies mainly focused on the axial heat transfer characteristics, and there is little research on circumferential heat transfer. Regarding circumferential heat transfer, Yang et al. analysed the influence of the circumferential slot structure of the electromagnetic stick on the bulging ability and bulging uniformity of RPECT [15]. The results showed that increasing the slot number and size can reduce the bulging value. Hajmohammadi et al. analysed the heat exchange capacity of array fins in a circular channel [16]. The results showed that the heat exchange capacity of a nonuniform fin structure can be increased by 46% compared with that of a traditional channel. Ding et al. analysed the heat dissipation characteristics of vertically oriented three-dimensional (3-D) finned tubes, and the results showed that the Nusselt number of tubes with such fins was 207% higher than that of smooth tubes [17]. The above studies revolve around the circumferential heat transfer capacity of the cylinder, but the involved objects are different from the ETCR. Considering the technical characteristics of ETCR, TEC is distributed on the roll inner wall as the temperature control device, forms different temperature fields and then makes the roll bulge. Therefore, the circumferential temperature difference can also cause the bulging difference.

Given the crucial influence of the ETCR circumferential characteristics on the roll profile control ability, an electronic temperature control model in the circumferential direction of the roll is established and verified

on the experimental platform. To analyse the difference in the circumferential regulation of the ETCR, this paper compares and analyses the different aspects of the ETCR: bulging ability, bulging difference, and temperature field distribution. In addition, the influence of roll structure parameters, TEC layout and TEC parameters on the electronic temperature control capability are also discussed, and the improvement methods are analysed.

2. Circumferential Problem Analysis Of Etcr

In the prediction of the ETCR roll profile, the roll can be divided into multiple TEC adjustment sections in the axial direction, and every section needs to be given a thermal boundary of the axisymmetric prediction model. In fact, TEC is often prepared in the form of a sheet rather than a ring. Therefore, the circumferential bulging of a TEC adjustment section is often jointly controlled by a plurality of TECs. Considering that the thermal boundary is not uniform at this time, it is necessary to equivalently simplify this thermal boundary. TEC usually adopts a layout with equal angular intervals in the circumferential direction in a TEC adjustment section. According to this feature, the concepts of single piece influence angle Deg_s, direct influence angle α_s and indirect influence angle β_s can be proposed. A schematic diagram of the structure is shown in Fig. 1. The single-piece influence angle Deg_s is the circumferential angle that a TEC is responsible for when n TECs are installed circumferentially in the roll inner wall. The calculation Formula (1) is as follows,

$$Deg_s = \frac{2\pi}{n} \tag{1}$$

The direct influence angle α_s is the circumferential angle corresponding to the TEC application area in a Deg_s. The calculation Formula (2) is as follows:

$$\alpha_s = \arcsin\frac{L}{2R} \tag{2}$$

where R is the roll radius and D_R is the roll diameter.

The indirect influence angle β_s is the circumferential angle corresponding to the no-TEC application area in a Deg_s. The calculation Formula (3) is as follows.

$$\beta_s = \frac{\pi}{n} - \arcsin\frac{L}{2R} \tag{3}$$

Figure 1 **Schematic diagram of TEC influence angle**

If the TEC control temperature is T_c the circumferential function of the heat source in the roll inner wall can be obtained according to the periodic distribution characteristics of the TEC layout, as shown in Formula (4).

$$f(\theta) = \begin{cases} T_c & \frac{2\pi}{n}(i-1) - k \le \theta \le \frac{2\pi}{n}(i-1) + k \\ 0 & \frac{2\pi}{n}(2i-3) \le \theta \le \frac{2\pi}{n}(i-1) - k \cup \frac{2\pi}{n}(i-1) + k \le \theta \le \frac{2\pi}{n}(2i-1) \end{cases}$$

4

Where, $i = 1, 2, 3, \ldots, n.$,$k = arcsin\frac{d}{2R}$, d is the length of the TEC.

According to Formula (4), the period of the periodic problem can be obtained $T = \frac{2\pi}{n}$,$a = \frac{j}{\pi} arcsin\frac{d}{2R}$. Ac, ording to the Fourier expansion (5), the Fourier expansion can be performed to obtain Formula (6).

$$f(\theta) = \begin{cases} 1 & |\theta| \le \frac{aT}{2} \\ 0 & |\theta| > \frac{aT}{2} \end{cases}$$

5

$$f(\theta) \sim \frac{a_0}{2} + \sum_{j=1}^{\infty} a_j \cos\left(\frac{2\pi jt}{T}\right) \qquad (6)$$

Where, $a_0 = \frac{2}{T}\int_{-\frac{aT}{2}}^{\frac{aT}{2}} f(\theta)\, d\theta = 2a$, $a_j = \frac{2}{T}\int_{-\frac{aT}{2}}^{\frac{aT}{2}} f(\theta)\cos\left(\frac{2\pi j\theta}{T}\right) d\theta = \frac{2}{j\pi}\sin(ja\pi)$.

Therefore, Formula (6) is further simplified, and Formula (7) is obtained.

$$f(\theta) \sim a + \frac{2}{\pi}\sum_{j=1}^{\infty} \frac{1}{j} \sin(ja\pi)\cos\left(\frac{2\pi j\theta}{T}\right) \qquad (7)$$

Where, j = 1, 2, 3, ……

The above formulas have the ability to solve the equivalent heat source. The heat sources of the TEC are periodically fixed on the roll inner wall, so the equivalent process easily ignores the thermal ratchet effect caused by the TEC distribution. If the thermal ratchet is so severe that it produces a corresponding

bulging ratchet, it can further affect the bulging effect of the ETCR. Therefore, it is necessary to analyse the influence of the ratchet of ETCR to determine the applicability of the equivalent relationship.

3. Circumferential Fe Model Of Etcr Establishment And Verification

3.1 Circumferential FE model of ETCR establishment

To analyse the influence law of the ratchet of ETCR, a circumferential FE model of ETCR is established, as shown in Fig. 2. Considering that the axial layout of the TEC is usually close-packed, the ETCR model can be simplified to a plane strain model. The model includes a TEC heat source, silicone grease, electronic temperature control roll and air unit. According to the principle of ETCR, the temperature of the TEC control terminal T_c can be adjusted based on the stable temperature of the TEC reference terminal T_r, and the dynamic adjustment of T_c can be realized by adjusting the TEC control current. The stability time for T_c is generally within 60 s, which is far less than the control time of the ETCR. Therefore, it can be assumed that T_c can reach the preset temperature at the initial state in the FE model of the ETCR. Therefore, T_c is applied to one end of the silicone grease in the form of a thermal boundary. The other end of the silicone grease is bonded to the electronic temperature control roll, which can transfer the heat of the TEC control terminal to the electronic temperature control roll. The specific parameters of the FE model are shown in Table 1.

Table 1
Parameters of the FE model

Parameter	Value	Parameter	Value
Roll diameter	140–420 mm	Hole diameter	80–120 mm
TEC size	40 mm × 40 mm	TEC thickness	5 mm
TEC control current	1–5 A	Silicone grease thickness	2 mm
TEC amount	3–5	TEC control time	1200 s
TEC control mode	Hot end control	Initial temperature	23 ℃

In the process of solid contact heat transfer, the heat transfer capacity is related to factors such as the pressure between two objects, the microscopic unevenness degree of the contact surface, and the effective contact area. Considering that the TEC and the roll are bonded with silicone grease, silicone grease has a certain viscosity and can effectively fill the area between the TEC and the roll. Therefore, the roll and silicone grease can be considered an adhesive contact. The contact heat transfer coefficient, which is equal to the thermal conductivity of the thermally conductive silicone grease, is 2.4 W/(m^2·K). The roll material is C45, the density is 7.85 g/cm^3, and the thermal property parameters are shown in Fig. 3. The roll is cooled through air cooling, and its heat transfer coefficient is 5 W/(m^2·K).

Figure 3 **Thermal property parameters of C45**

3.2 FE model verification

An experimental ETCR platform is built and used to measure circumferential bulging in different cases, as shown in Fig. 4. The platform includes a DC power supply, detection channel, ETCR, strain gauge, test system, regulating current device and cooling water tank. In the platform, strain gauges are applied on the ETCR in the manner shown in Fig. 4(b), which can be used to measure the circumferential strain of the roll. Figure 4(c) shows the changes in the strain gauges before and after roll bulging. According to the geometric relationship, the geometric relationship before and after deformation is Formula (8) and Formula (9).

$$R\theta = L$$

8

$$(R + \Delta R)\,\theta = L + \Delta L$$

9

where R is the roll radius before bulging; ΔR is the radial bulging amount of the roll, and its value is equal to $\varepsilon_r R$; ε_r is the radial strain; L is the length of the strain gauge before bulging; ΔL is the stretching amount of the strain gauge, and its value is equal to $\varepsilon_c L$; ε_c is the radial strain; and θ is the central angle corresponding to the length of the strain gauge.

Formula (8) and Formula (9) are combined to obtain Formula (10).

$$\epsilon_r = \epsilon_c$$

10

Therefore, the radial bulging amount of the roll can be obtained from the actual measured value of the strain gauge. TECs are assembled on the electronic temperature control ring, as shown in Fig. 4(d), installed in the middle of the roll inner wall. The outer ring surface of the electronic temperature control ring can be equipped with multiple TECs along the circumferential direction, and the inner ring is a cooling water path through which cooling water can flow, as shown in Fig. 4(e). The silicone grease marked with bright colour in Fig. 4(e) is used for bonding between the TEC and the roll inner wall to ensure the heat transferability of the TEC to the roll.

Figure 4 **Experimental platform of ETCR and detection principle**

Based on the above experimental platform, the roll diameter is φ140 mm, the roll inner wall diameter is 100 mm, and the roll length is 300 mm. TEC adopts 5 pieces in the circumferential direction of the roll, which are spliced on the electronic temperature control ring and installed in the middle of the roll inner wall. The experimental conditions were as follows: the ambient temperature was 20°C, the cooling water temperature was 18°C, the TEC control current was 3 A, and the control time was 1200 s. Figure 5 is a

comparison diagram of the experiment and simulation of the maximum radial bulge of the roll. The results show that the maximum bulging amount can increase rapidly in the early stage of regulation and gradually stabilize. In the first 15 minutes, the experimental result is slightly lower than the simulated result, and the difference between the two is within 1.3 μm. After the first 15 minutes, the difference between the experiment and the simulation was reduced to 0.5 μm. The reason for the difference is that the model considers that the TEC is completely attached to the roll inner wall, but in the experiment, there is a certain gap due to the paste, which causes the heat transfer effect of the experiment to be inferior to the simulation effect and causes the difference between the two. However, overall, the two trends are basically the same. The experimental results no longer increase before and after 20 minutes, which can be considered at steady-state conditions. More experiments have been carried out on the platform with similar results as shown in Fig. 4. Therefore, the FE model has a certain simulation accuracy and can be applied to ETCR research.

In addition, according to the results in Fig. 5, at 1200 s, the electronic temperature control roll enters a steady-state, while T_c has already entered a steady-state at this time. Therefore, the variation in T_c with the TEC control current when T_r is 18°C is shown in Fig. 6. The results show that the TEC control currents from 1 A to 5 A correspond to T_c values of 35 ℃, 50 ℃, 78 ℃, 116 ℃, and 152 ℃.

4 Results

4.1 The diameter of the roll and the diameter of the roll inner hole

To analyse the influence of the TEC layout on the bulging uniformity, the maximum bulging difference is defined as the C_{ED}, which is the difference between the maximum and minimum bulging amounts in the radial direction of the roll, and the calculation formula is shown in Formula (11).

$$C_{ED} = C_{max} - C_{min}$$

11

where C_{max} is the maximum bulging amount and C_{min} is the minimum bulging amount.

Figure 7 shows the variation of C_{max} and C_{ED} with D_R under different Deg_s. The T_c is 50°C in these cases, and a uniform heat flow condition is established to provide a reference. In the uniform case, the element edges on the roll inner wall are set as the first thermal boundary with a value of 50 ℃. In Fig. 7 (a), C_{max} can be increased with increasing D_R and has similar change laws under different Deg_s. The law can be described as follows: with increasing D_R, the increasing rates of C_{max} gradually decrease. After the D_R reaches 420 mm, C_{max} begins to stabilize and no longer increases as the D_R increases. Compared with the cases of different Deg_s, when Deg_s is decreased from 120° to 60°, C_{max} can be gradually increased. Meanwhile, the influence value of D_R on C_{max} is 6.97 μm, 8.53 μm, 9.56 μm, and 10.3 μm, and the value is

10.88 μm in the uniform case. In Fig. 7 (b), C_{ED} can be gradually decreased as D_R increases. When D_R is large enough, C_{ED} is almost 0 μm. When the D_R is small, the unevenness of roll bulging is more serious, and the larger the Deg_s is, the more obvious the bulging ratchet effect of ETCR. When Deg_s is reduced from 120° to 60°, the maximum C_{ED} values are 3.87 μm, 0.88 μm, 0.49 μm, and 0.09 μm, respectively. After Deg_s is reduced to 90°, the C_{ED} is less than 1 μm.

Figure 7 **Variation in** C_{max} **and** C_{ED} **with increasing** D_R **under different** Deg_s

In the ETCR, the reason for the roll profile variation is that the internal heat source changes the temperature field of the roll and further changes the thermal bulging effect. Therefore, the ratchet characteristic of the ETCR is related to the temperature field distribution. According to the result in Fig. 7, a severe bugling ratchet exists in the case with Deg_s = 120°. To select the evaluation criterion of the ratchet, the roll internal temperature fields with serious bulging ratchets are extracted, as shown in Fig. 8. Compared with the results in Fig. 8, the temperature range above 28°C can reflect the thermal ratchet of the ETCR. Considering that the corresponding cases in Fig. 8 are the worst cases of roll bulging uniformity, 28°C can be selected as the lowest temperature value of the thermal ratchet.

Figure 8 **Roll internal temperature fields when** Deg_s **is 120°**

Figure 9 shows the variation of the 28℃ temperature-affected zone inside the roll with D_R under different Deg_s. The results show that with increasing Deg_s, the thermal ratchet is alleviated, which is consistent with the result in Fig. 7 (b). With a smaller D_R, reducing Deg_s can alleviate the thermal ratchet problem caused by the TEC layout to a certain extent. When Deg_s is 60°, the thermal ratchet degree is lower, and uniform heat flow on the roll inner wall can be realized. With a larger roll diameter, except for the case where Deg_s is 120°, the ratcheting phenomenon of the temperature field in other cases can basically be eliminated.

Figure 9 **Variation in the 28°C temperature-affected zone under different** D_R

To further evaluate the thermal ratchet degree, the circumferential unit temperature rise control quantity is defined as ΔT. ΔT is the ratio of the temperature difference to Deg_s, and can be calculated by Formula (12).

$$\Delta T_c = \frac{T_{Deg-max} - T_{Deg-min}}{Deg_s}$$

12

where $T_{Deg-max}$ is the maximum temperature value within Deg_s, and $T_{Deg-min}$ is the minimum temperature value within Deg_s.

Figure 10 shows the change in ΔT of the inner wall and outer wall of the roll with changing D_R under different Deg_s. In Fig. 10(a), ΔT can be decreased as D_R increases, and the rate of decrease can be gradually decreased. Under the same D_R, ΔT can be increased with increasing Deg_s. When *Degs* is changed from 60° to 120°, ΔT can be gradually increased with increasing D_R, which indicates that increasing Deg_s can cause the ratchet phenomenon on the roll inner wall to become more serious. In Fig. 10 (b), the change in ΔT can be divided into two stages: the first stage is [140 mm, 220 mm], ΔT can be decreased rapidly with increasing D_R, and the rate of decrease slowly declines. The second stage is [220 mm, 420 mm], the decrease rate declines further and finally stabilizes, and with the continuous increase in D_R, ΔT finally approaches 0 ℃/°. Similarly, under the same D_R, the increase in Deg_s can increase ΔT. When D_R is 140 mm and Deg_s decreases from 120° to 60°, ΔT can decrease from 0.03 ℃/° to 0.01 ℃/°. The larger the Deg_s is, the larger the drop is. When Deg_s is 120°, the maximum drop is 0.03 ℃/°.

Figure 10 **Variation in** ΔT **of the inner and outer walls of the roll with changing** D_R **under different** Deg_s

According to the above results, when Deg_s exceeds 90°, the ratio of β/α is too great, and the thermal ratchet phenomenon of the roll and the maximum difference value of roll bulging are both large, which is not suitable for ETCR. When Deg_s is less than 90°, the maximum difference value of roll bulging is small, and it can be further reduced by increasing D_R, so it is suitable for ETCR.

In addition to the roll diameter, the diameter of the roll inner wall D_{IH} is also a parameter that can affect the effectiveness of the ETCR. In Fig. 7, the cases where D_R is 260 mm have good bulging ability and small C_{ED} and can be selected as the basic condition. To analyse the influence of D_{IH} on ETCR, D_{IH} and Deg_s are changed to analyse the bulging ability. Figure 11 shows the variation of C_{max} and C_{ED} with D_{IH} under different Deg_s. The results in Fig. 11 (a) show that with the increase of D_{IH}, C_{max} can be decreased, and the decrease rate of C_{max} is the same under different Deg_s. Under the same D_{IH}, the increase in Deg_s can reduce C_{max}. When Deg_s is increased from 72° to 120°, the change in C_{max} with increasing D_{IH} is -1.13 μm, -1.37 μm, and − 1.4 μm. On the whole, under the same T_c, changing D_{IH} has a small influence on C_{max}, and the influence value is less than 2 μm. The results in Fig. 11 (b) show that C_{ED} gradually increases with increasing D_{IH}. When Deg_s is 120°, the increased value of C_{ED} is the largest, and the value is 1.48 μm. When the Deg_s are 90° and 72°, the change values of C_{ED} are 0.29 μm and 0.11 μm, respectively.

Figure 11 **Variation in** C_{max} **and** C_{ED} **with increasing** D_{IH} **under different** Deg_s

In addition, the results in Fig. 11 (a) also show that the change trend of C_{max} in the uniform case is different from those in other cases. C_{max} can be gradually increased with increasing D_{IH} in the uniform case, while C_{max} can be decreased with increasing D_{IH} in the other cases. The case with Deg_s of 120° is the most serious. To analyse the reason, the node temperature, which is located in the radial path from

the roll inner wall to the maximum bulging point of the roll surface, is extracted when Deg_s is 120°, as shown in Fig. 12. The results show that the larger the D_{IH} is, the lower the point temperature at the same distance from the roll inner wall, so the corresponding thermal bulge is lower at the same position. The reason is that under a constant roll diameter, the expansion of D_{IH} is equivalent to reducing the roll wall thickness. The area close to the roll surface can obtain a higher temperature and form a larger thermal bulge. However, this law exists when there is no difference or a small difference in the roll circumferential temperature. When the heat source is uniformly distributed in the circumferential direction, the bulging ability can be improved by decreasing the roll wall thickness. In addition to the uniform case, the heat source is nonuniform in the circumferential direction, so increasing D_{IH} reduces the roll wall thickness and increases the distances among TECs. For two adjacent TECs, the symmetry plane between two TECs is also the symmetry plane of the heat transfer influence zone. With increasing D_{IH}, the circumferential heat transfer between the adjacent TEC is also more obvious, which leads to a decrease in C_{max}.

Figure 13 shows the internal temperature fields of the roll with changing D_{IH}. The results show that in Fig. 13(a), (d), and (g), when Deg_s is 120°, regardless of the D_{IH} value, there is a severe thermal ratchet problem in the internal temperature field of the roll. When Deg_s is reduced to 100°, the temperature ratchet is relieved, but when D_{IH} is larger, such as Fig. 13 (h), there is still a severe thermal ratchet. If Deg_s is further reduced, the thermal ratchet in the case in which the D_{IH} is 120 mm can also be relieved. The above changes are because the reduction in Deg_s can increase the total direct influence angle, so the input heat flow distribution on the roll inner wall is more uniform. In addition, it is not easy to produce thermal ratchet. When D_{IH} is increased, the total direct influence angle can be decreased and the indirect influence angle can be increased, so the uniformity of the input heat flow can be decreased on the roll inner wall, and the thermal ratchet effect is aggravated.

Figure 13 **Variation of the roll temperature field under different** D_{IH} **and** Deg_s

Figure 14 shows the change in ΔT of the inner and outer walls with D_{IH} under different Deg_s. In Fig. 14 (a), the ΔT of the inner wall of the roll can be increased with increasing D_{IH}, but the growth rate gradually decreases. Under the same D_{IH}, the larger the Deg_s, the larger the ΔT, and the worse the uniformity of the heat flow in the roll inner wall. In Fig. 14 (b), the ΔT of the roll outer wall can also be increased with increasing D_{IH}, but the growth rate gradually increases. The difference in the growth rate of ΔT between Fig. 14 (a) and (b) is that increasing D_{IH} can reduce the distance between the heat source and the roll surface, and the thermal ratchet caused by different Deg_s is more likely to appear on the outer wall of the roll.

Figure 14 **Variation in** ΔT **of the inner and outer walls of the roll with changing** D_{IH} **under different** Deg_s

In summary, increasing D_R can increase C_{max} and decrease C_{ED}, while increasing D_{IH} can decrease C_{max} and increase C_{ED}. Changing Deg_s can affect the effects of D_R and D_{IH}. Comparing the results of Fig. 7(b) and Fig. 11(b), the cases in which Deg_s is less than 90° have a relatively small maximum difference value

of roll bulging, so these cases are more suitable for ETCR than the cases in which Deg_s is more than 90°. Because Deg_s is the parameter of TEC, it is necessary to further analyse the influence of TEC parameters on the effect of ETCR.

4.2 The TEC control temperature

According to previous research results, the bulging control effect of the roll is more obvious and C_{ED} is small when D_R is 260 mm and D_{IH} is 100 mm. Therefore, these parameters are selected to analyse the influence of T_c on the thermal ratchet effect. Figure 15 shows the variation of C_{max} and C_{ED} with T_c under different Deg_s. The results show that both C_{max} and C_{ED} can increase linearly with increasing T_c. In Fig. 15(a), when Deg_s is reduced from 120° to 60°, the growth rate of C_{max} is 0.25 μm/℃, 0.32 μm/℃, 0.38 μm/℃, and 0.43 μm/℃. Compared with the uniform case of 0.48 μm/℃, the smaller the value of Deg_s is, the closer the bulging effect of the roll is to the uniform case. In Fig. 15(b), in addition to the case in which Deg_s is 120°, other cases have lower C_{ED}. When Deg_s is decreased from 90° to 60°, the variation rate of C_{ED} is 0.005 μm/℃, 0.001 μm/℃, and 0.0001 μm/℃. The results indicate that cases in which Deg_s are 90°, 72°, and 60° can meet the requirements of uniform circumferential bulging.

Figure 15 **Variation in** C_{max} **and** C_{ED} **with increasing** T_c **under different** Deg_s

Figure 16 shows the changes in the 28℃ temperature-affected zone with T_c under different Deg_s. The results show that when Deg_s is 120°, only the case with a larger T_c has a relatively small circumferential difference in the temperature field. In comparison, a case with a lower T_c has a more severe thermal ratchet phenomenon. Compared to the results in Fig. 15(b), even if T_c is increased, the cases with Deg_s of 120° are still not suitable as an optional form of TEC layout. When Deg_s is 90°, 72°, and 60°, the thermal ratchet phenomenon occurs only when the TEC control temperature is small, and the thermal ratchet phenomenon is eliminated after slightly increasing T_c.

Figure 16 **Variation of the 28℃ temperature-affected zone with** T_c **under different** Deg_s

Figure 17 shows the change in ΔT of the inner and outer walls of the roll with T_c under different Deg_s. The results show that the ΔT of the outer wall and inner wall also increases linearly with increasing T_c. In Fig. 17 (a), the growth rate of ΔT increases with increasing Deg_s, but the difference is not large. In the cases, the growth curves of Deg_s 90° and 120° almost coincide in value and trend, indicating that the heat flow uniformities of the roll inner wall under the two cases are approximately the same. On the other hand, under the same T_c, ΔT can be increased with increasing Deg_s, and the heat flow uniformity of the roll inner wall is worse. In Fig. 17 (b), the change value of ΔT in the roll outer wall with changing T_c is much smaller than that of the roll inner wall. The change rule of ΔT with T_c and Deg_s is the same as in Fig. 17(a). Therefore, in the cases of different T_c, the temperature uniformity of the roll inner wall is greatly affected by T_c, while the influence on the roll outer wall is very small. For the roll inner wall

temperature, the increase in T_c and Deg_s can lead to an increase in the circumferential unevenness of the roll inner wall temperature.

Figure 17 **Variation in** ΔT **of the inner and outer walls of the roll with changing** T_c **under different** Deg_s

4.3 The single piece influence angle

In addition to T_c, the TEC amount is also an important parameter of TEC. The electronic temperature-controlled roll's circumferential sheet-carrying capacity is related to the diameter of the inner hole of the roll. Therefore, the parameters of the FE model are as follows: D_R is selected as 260 mm, D_{IH} is 80 mm, 100 mm, and 120 mm, and T_c is selected as 50°C. Figure 18 shows the variation in C_{max} and C_{ED} with Deg_s under different D_{IH}. The results showed that under different D_{IH}, C_{max} can be decreased and C_{ED} can be increased with increasing Deg_s. The change in C_{ED} is divided into two stages: when Deg_s is [40°, 90°], the difference in C_{ED} under different D_{IH} is small. It can be considered that changing D_{IH} cannot affect the effect of Deg_s on the radial bulging unevenness. When Deg_s exceeds 90°, the greater the D_{IH} is, the more serious the radial bulging unevenness of the roll.

Figure 18 **Variation of** C_{max} **and** C_{ED} **with** Deg_s **under different** D_{IH}

Figure 19 shows the variation in the roll internal temperature field under different D_{IH} and Deg_s. The results show that, regardless of D_{IH}, with the increase in Deg_s, the thermal ratchet phenomenon can become increasingly obvious. Especially when Deg_s is 120°, the thermal ratchet phenomenon is so obvious that it affects the roll bulging ability and the circumferential uniformity of the roll bulging. Meanwhile, this effect can further increase as D_{IH} increases. It can be seen from the temperature field distribution that the smaller the D_{IH} is, the greater the Deg_s demand value that can ensure uniform bulging is. For example, for a case in which D_R is 80 mm, the Deg_s demand value is 90°; for a case in which D_R is 100 mm, the Deg_s demand value is 72°; and for a case in which D_R is 120 mm, the Deg_s demand value is 60°.

Figure 19 **Variation of the roll temperature field under different** D_{IH} **and** Deg_s

Figure 20 shows the change in ΔT of the inner and outer walls of the roll with changing Deg_s under different D_{IH}. In Fig. 20(a), the changing trend of ΔT can be described as "increasing first and then becoming stable." The smaller the D_{IH} is, the smaller the ΔT on the inner wall of the roll, and the better the uniformity of the inner wall heat flow. In Fig. 20 (b), ΔT increases with Deg_s, but its value is much smaller than that in Fig. 20(a); that is, the ΔT in the roll outer wall is smaller, and the temperature distribution is more uniform.

Figure 20 **Variation in** ΔT **of the inner and outer walls of the roll with changing** Deg_s **under different** $_{DIHs}$

4.4 The copper layer

The above research shows that due to the influence of the bulging ratchet and the thermal ratchet, the case in which Deg_s is 120° cannot be suitable for ETCR. The main reason is the uneven temperature distribution of the circumferential direction. To improve this problem, a metal layer with high thermal conductivity can be arranged on the inner hole of the roll so that the heat source provided by TEC is uniform on the inner hole of the roll. In this paper, the beryllium copper layer is used as the metal layer of the roll inner hole, the thermal conductivity is 198 W/(m·K), and the value range of the layer thickness H_{Cu} is 0 mm to 12 mm. Figure 21 shows the variation in C_{max} and C_{ED} with T_c under different H_{Cu} values. The results show that the increase in the beryllium copper layer has almost no effect on C_{max}, but it can change the circumferential difference of the roll bulging. In Fig. 21, the application of the beryllium copper layer can effectively reduce the C_{ED} to 2 μm. If H_{Cu} is further increased, C_{ED} can be reduced by a small margin.

Figure 21 **Variation in C_{max} and C_{ED} with increasing T_c under different H_{Cu}**

Figure 22 shows the change in ΔT of the inner and outer walls of the roll with changing T_c under different H_{Cu} values. In Fig. 22 (a), ΔT can be decreased with increasing H_{Cu}, indicating that the thermal ratchets near the roll inner wall have been well improved. In Fig. 22 (b), the influence of H_{Cu} on ΔT is the same as that in Fig. 22 (a), but the variation magnitude of ΔT is much smaller than that in Fig. 22(a). On the whole, by adding a thermally conductive metal layer to the roll inner wall, the thermal ratchet can be improved, thereby reducing C_{ED} and improving the availability of the ETCR.

Figure 22 **Variation in ΔT of the inner and outer walls of the roll with changing T_c under different H_{Cu}**

5. Conclusion

In this paper, for the circumferential bulging capacity and uniformity, the maximum bulging amount, the maximum bulging difference and the roll temperature field are analysed, and the effects of different parameters are discussed. The conclusions obtained are as follows:

(1) For the structure parameters of the roll, the increases of the roll diameter and the decrease of the diameter of the roll inner hole can increase the maximum bulging amount, decrease the maximum bulging difference. Meanwhile, the variation of the diameters can change the roll temperature field to decrease the difference of the circumferential temperature. Therefore, the roll diameter and the diameter of the roll inner hole need to be matched reasonably to give full play to the ability of ETCR.

(2) For the TEC layout, the increase of the TEC control temperature and the decrease of the single piece influence angle can increase the maximum bulging amount and improve the temperature ratchet. The effect of changing the single piece influence angle on the bulging uniformity is larger than that of the temperature of TEC. When the single piece influence angle is too large, the temperature ratchet is more serious and cannot even be used for the roll profile control of ETCR.

(3) To solve the problem that the case with a large single piece influence angle can not be used, adding an inner hole layer of a high thermal conductivity material is proposed to be used for improving the temperature ratchet in this paper. Through simulation analysis, the copper layer has little influence on the bulging ability of the roll and can reduce the circumferential bulging difference.

Declarations

Funding

This work was supported by the Natural Science Foundation of China in Hebei Province (Grant No. E2021203129) for the support to this research.

Declaration of Interest Statement

The authors declare that they have no known competing financial interests or personal relationships that could have appeared to influence the work reported in this paper.

Author contributions

The analysis of bulging ability, temperature field were done by Tingsong Yang and Zhiqiang Xu; FE model establishment and FE model Validation were carried out by Tingsong Yang and Haonan Zhou; Experimental platform was built by Yang Hai with the support of Zhiqiang Xu and Fengshan Du; Tingsong Yang revised the paper. All authors have read and agreed to the published.

References

[1] C. Lu, A.K. Tieu, Z.Y. Jiang, A design of a third-order CVC roll profile, Journal of Materials Processing Technology 125 (2002) 645-648. https://doi.org/10.1016/S0924-0136(02)00373-4

[2] H.B. Li, J. Zhang, J.G. Cao, L.L. Meng, Analysis of Crown Control Characteristics for Smart Crown Work Roll, Advanced Materials Research 156-157 (2011) 1261-1265. http://doi.org/10.4028/www.scientific.net/AMR.156-157.1261

[3] J.G. Cao, G.C. Wei, J. Zhang, X.L. Chen, Y.Z. Zhou, VCR and ASR technology for profile and flatness control in hot strip mills, Journal of Central South University of Technology 15(002) (2008) 264-270. http://doi.org/10.1007/s11771-008-0049-0

[4] X.C. Wang, Q. Yang, Y.Z. Sun, Rectangular Section Control Technology for Silicon Steel Rolling, Journal of Iron and Steel Research International, 22(3) (2015) 185-191. https://doi.org/10.1016/S1006-706X(15)60028-0

[5] T. Masui, J. Yamada, T. Nagai, T. Nishino, Strip Shape and Profile Control with a New Type of the Variable Crown Roll System, Transactions of the Iron and Steel Institute of Japan 23(10) (1983) 846-853.

https://doi.org/10.2355/isijinternational1966.23.846

[6] Q.D. Zhang, W.G. Wang, X.M. Zhou, X.K. Zhou, Flatness control behavior of a DSR mill for wide steel strips, Journal of Beijing University of science and technology 01 (2008) 71-76. https://doi.org/10.13374/j.issn1001-053x.2008.01.006

[7] Sumitomo Metal Ind, (1994). Shape controller in sheet rolling. JP patent, 6015319A. 01–25.

[8] W.W. Liu, Y.F. Feng, T.S. Yang, F.S. Du, J.N. Sun, Analysis of the induction heating efficiency and thermal energy conversion ability under different electromagnetic stick structures in the RPECT, Applied Thermal Engineering 145 (2018) 277-286. https://doi.org/10.1016/j.applthermaleng.2018.09.043

[9] A.F.M. Arif, O. Khan, A.K. Sheikh, Roll deformation and stress distribution under thermo-mechanical loading in cold rolling, Journal of Materials Processing Technology 147(2) (2004) 255-267. https://doi.org/10.1016/j.jmatprotec.2004.01.005

[10] X.L. Zhang, J. Zhang, X.Y. Li, H.X. Li, G.C. Wei, Analysis of the thermal profile of work rolls in the hot strip rolling process, Journal of Beijing University of science and technology 11 (2004) 173-177. https://doi.org/10.1016/j.jmps.2003.08.002

[11] C.M. Park, J.T. Choia, H.K. Moona, G.J. Park. Thermal crown analysis of the roll in the strip casting process, Journal of Materials Processing Technology 209 (2009) 3714-3723. https://doi.org/10.1016/j.jmatprotec.2008.08.029

[12] D. Benasciutti, E. Brusa, G. Bazzaro. Finite element prediction of thermal stresses in work roll of hot rolling mills. Procedia Engineering 2 (2010) 707-716.

[13] M. Jiang, X. Li, J. Wu, G. Wang, A precision on-line model for the prediction of thermal crown in hot rolling processes, International Journal of Heat & Mass Transfer 78 (2014) 967-973. https://doi.org/10.1016/j.ijheatmasstransfer.2014.07.061

[14] S.X. Chen, W.G. Li, X.H. Liu, Thermal Crown Model and Shifting Effect Analysis of Work Roll in Hot Strip Mills, Journal of Iron and Steel Research (International) 22 (2015) 777-784. https://doi.org/10.1016/S1006-706X(15)30071-6

[15] T.S. Yang, J.Y. Liu, H.N. Zhou, Z.Q. Xu, F.S. Du, Analysis of the thermal-force roll profile control ability under different hole structures and slot structures in the RPECT, The International Journal of Advanced Manufacturing Technology 116 (2021) 403-415. https://doi.org/10.1007/s00170-021-07399-3

[16] M.R. Hajmohammadi, A. Doustahadi, M. Ahmadian-Elmi, Heat transfer enhancement by a circumferentially non-uniform array of longitudinal fins assembled inside a circular channel. International Journal of Heat and Mass Transfer 158 (2020) 120020. https://doi.org/10.1016/j.ijheatmasstransfer.2020.120020

[17] Y.D. Ding, W.H. Deng, B. Ding, Y.H. Gu, Q. Liao, Z.Z. Long, X. Zhu, Experimental and numerical investigation on natural convection heat transfer characteristics of vertical 3-D externally finned tubes, Energy 239 (2021) 122050. https://doi.org/10.1016/j.energy.2021.122050

Figures

Figure 1

Schematic diagram of TEC influence angle. (a) TEC layout, and (b) TEC influence angles

Figure 3

Thermal property parameters of C45. (a) Thermal conductivity, and (b) Specific heat

Figure 4

Experimental platform of ETCR and detection principle

(a) Experimental platform of the ETCR, (b) TEC layout, (c) schematic diagram of circumferential/radial elongation before and after bulging, (d) assembly diagram of the electronic temperature control ring, (e) schematic diagram of the electronic temperature control ring, and (f) profile diagram of the electronic temperature control roll

Figure 5

Comparison diagram of the experiment and simulation of the maximum radial bulge

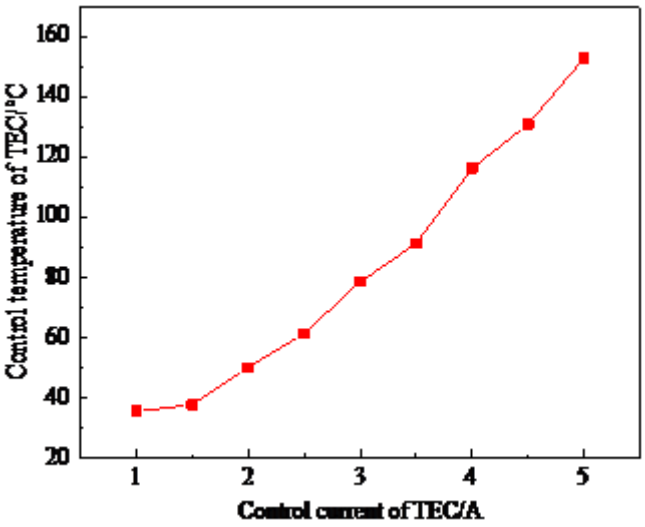

Figure 6

Variation of T_c with the TEC control current when T_r is 18 ℃

Figure 7

Variation in C_{max} and C_{ED} with increasing D_R under different Deg_s. (a) C_{max}, and (b) C_{ED}

Figure 8

Roll internal temperature fields when Deg_s is 120°. D_R is (a) 140 mm, (b) 260 mm, and (c) 420 mm

Figure 9

Variation in the 28℃ temperature-affected zone under different *DR*

Deg_s are (a) 120°, (b) 90°, (c) 72°, and (d) 60°

Figure 10

Variation in ΔT of the inner and outer walls of the roll with changing D_R under different Deg_s

(a) the roll inner wall, and (b) the roll outer wall

Figure 11

Variation in C_{max} and C_{ED} with increasing D_{IH} under different Deg_s

(a) C_{max}, and (b) C_{ED}

Figure 12

Node temperatures located in the radial path from the roll inner wall to the maximum bulging point of the roll surface

Figure 13

Variation of the roll temperature field under different D_{IH} and Deg_s

(a)-(c) D_{IH} is 80 mm and Deg_s is from 120° to 72°, (d)-(f) D_{IH} is 100 mm and Deg_s is from 120° to 72°, (g)-(i) D_{IH} is 120 mm and Deg_s is from 120° to 72°

Figure 14

Variation in ΔT of the inner and outer walls of the roll with changing D_{IH} under different Deg_s

a) the roll inner wall, and (b) the roll outer wall

Figure 15

Variation in C_{max} and C_{ED} with increasing T_c under different Deg_s

(a) C_{max}, and (b) C_{ED}

Figure 16

Variation of the 28℃ temperature-affected zone with T_c under different Deg_s

Deg_s is (a) 120°, (b) 90°, (c) 72°, and (d) 60°

Figure 17

Variation in ΔT of the inner and outer walls of the roll with changing T_c under different Deg_s

(a) the roll inner wall, and (b) the roll outer wall

Figure 18

Variation of C_{max} and C_{ED} with Deg_s under different D_{IH}

(a) C_{max}, and (b) C_{ED}

Figure 19

Variation of the roll temperature field under different D_{IH} and Deg_s

(a)-(c) D_{IH} is 80 mm and Deg_s is from 72° to 120°, (d)-(f) D_{IH} is 100 mm and Deg_s is from 60° to 120°, (g)-(i) D_{IH} is 120 mm and Deg_s is from 45° to 120°

Figure 20

Variation in ΔT of the inner and outer walls of the roll with changing Deg_s under different $_{DIHs}$

(a) the roll inner wall, and (b) the roll outer wall

Figure 22

Variation in ΔT of the inner and outer walls of the roll with changing T_c under different H_{Cu}

(a) the roll inner wall, and (b) the roll outer wall